Are Brønsted Acids the True Promoter of Metal-Triflate-Catalyzed Glycosylations? A Mechanistic Probe into 1,2-*cis*-Aminoglycoside Formation by Nickel Triflate

Eric T. Sletten,[†] Yi-Jung Tu,[‡] H. Bernhard Schlegel,*,[‡] and Hien M. Nguyen*,[‡]

[†]Department of Chemistry, University of Iowa, Iowa City, Iowa 52242, United Sates
[‡]Department of Chemistry, Wayne State University, Detroit, Michigan 48202, United States

S *Supporting Information*

ABSTRACT: Metal triflates have been utilized to catalytically facilitate numerous glycosylation reactions under mild conditions. In some methods, the metal triflate system provides stereocontrol during the glycosylation, rather than the nature of protecting groups on the substrate. Despite these advances, the true activating nature of metal triflates remains unclear. Our findings indicated that the *in situ* generation of trace amounts of triflic acid from metal triflates can be the active catalyst species in the glycosylation. This fact has been mentioned previously in metal-triflate-catalyzed glycosylation reactions; however, a thorough study on the subject and its implications on stereoselectivity has yet to be performed. Experimental evidence from control reactions and ^{19}F NMR spectroscopy have been obtained to confirm and quantify the triflic acid released from nickel triflate, for which it is of paramount importance in achieving a stereoselective 1,2-*cis*-2-amino glycosidic bond formation via a transient anomeric triflate. A putative intermediate resembling that of a glycosyl triflate has been detected using variable temperature NMR (^1H and ^{13}C) experiments. These observations, together with density functional theory calculations and a kinetic study, corroborate a mechanism involving triflic-acid-catalyzed stereoselective glycosylation with *N*-substituted trifluoromethylbenzylideneamino-protected electrophiles. Specifically, triflic acid facilitates formation of a glycosyl triflate intermediate which then undergoes isomerization from the stable α-anomer to the more reactive β-anomer. Subsequent S_N2-like displacement of the reactive anomer by a nucleophile is highly favorable for the production of 1,2-*cis*-2-aminoglycosides. Although there is a previously reported work regarding glycosyl triflates, none of these reports have been confirmed to come from the counterion of the metal center. Our work provides supporting evidence for the induction of a glycosyl triflate through the role of triflic acid in metal-triflate-catalyzed glycosylation reactions.

KEYWORDS: *glycosylation mechanism, hidden Brønsted acid, kinetics, 1,2-cis-aminoglycosides, nickel triflate*
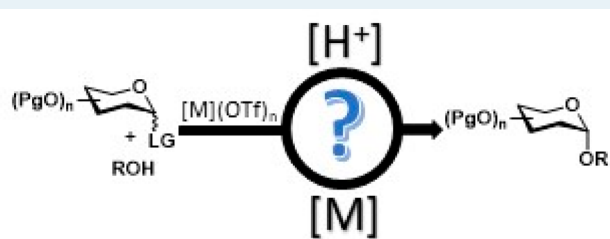
INTRODUCTION

Recent advances in the field of glycoscience have revealed carbohydrates as an essential component of many biologically important molecules in nature.[1] Carbohydrate oligosaccharides are often found in low concentrations and heterogeneous forms, greatly complicating their isolation and analysis. To attain these carbohydrate targets under mild and operationally simple techniques, many methodologies have begun to utilize catalytic amounts of transition metals.[2−4] Of these transition metal catalysts, metal triflates in particular have been found to be highly efficient at facilitating glycosylation reaction, and some even provide stereocontrol during the glycosylation.[2−7] Metal triflates have illustrated many advantages over traditional activating reagents for promoting glycosidic bond formation. Since the turnover is high, only substoichiometric amounts of metal triflates have been utilized in the reaction, thus promoting the strategies of "green chemistry".[8] Furthermore, the stereoselectivity of the newly formed glycosidic bond can be tuned by the nature of the ligand attached to the metal

center. In addition, transition metal complexes have been utilized to promote chemoselective activation for orthogonal glycosylation strategies.[2,3] However, during many of the mechanistic elucidations, the question remains for the true role of the metals in the catalytic glycosylations.

Recently, it has been presented that many organic transformations performed by metal triflate catalysts are truly promoted by triflic acid, which is released from the metal center and has been coined as "hidden Brønsted acid catalysis".[9−14] Although eluted in the literature,[15−22] a systematic study on the possible release of triflic acid from a metal triflate to promote a glycosylation has not yet been reported. Not only can the release of triflic acid potentially activate the departure of the anomeric leaving group, but there is also a possibility that it has implications on the stereo-

selectivity of the reaction, as it has been reported that the triflate anion can play an important role in the diastereoselectivity of the newly formed glycosidic bond.[23] However, the possibility that triflic acid plays a key role in catalytic glycosylations is quickly dismissed because studies by our group and others have illustrated that triflic acid was not able to replicate the results obtained by the metal triflate. Typically, the carbohydrate coupling products are obtained in poor yield using triflic acid with an equivalent amount to that of the metal triflate, leading to the impression that triflic acid is less effective and can be prematurely ruled out as the active catalyst.[6,11] To study the concept of "hidden Brønsted acid catalysis" being the actual promoter for metal-triflate-catalyzed glycosylation reactions and its impact on the stereoselectivity, we systematically probed the activation and operative mechanisms of our recently developed method for 1,2-cis-aminoglycoside synthesis via nickel-triflate-catalyzed glycosylation with a C(2)-benzylideamino N-phenyl trifluoroacetimidate electrophile (Scheme 1).[24]

Scheme 1. Formation of 1,2-cis-2-Aminoglycosides
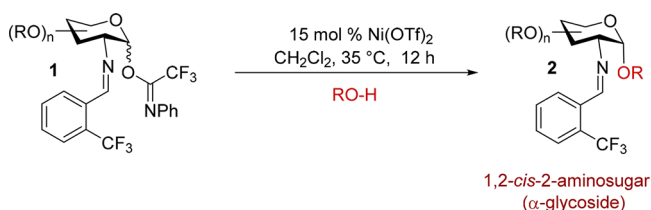
Herein, we report our detailed investigations of the 1,2-cis-2-amino glycosylation reaction aimed at understanding the mechanism of α-selective glycosidic bond formation utilizing nickel(II) triflate. Although the hidden Brønsted acid theory has been suggested previously, there are many discrepancies and lapses in the literature pertaining to a detailed study on the subject. Therefore, this work includes (1) confirming that the actual active catalyst species in the reaction can be triflic acid when utilizing metal triflate catalysts, (2) utilizing computational and experimental studies to detect and analyze transient glycosyl intermediates after N-phenyl trifluoroacetimidate activation by the "hidden Brønsted acid" released from Ni(OTf)$_2$, and (3) validating the significant role of the metal's

counterion on selectivity and activation. More importantly, this mechanistic study can have implications on future metal-catalyzed glycosylations and also to previously developed metal-catalyzed mechanisms, of which many contain triflate counterions, and a complementary glycosylation reaction can be performed under Brønsted acid conditions.

■ RESULTS AND DISCUSSION

As part of the effort to develop catalytic stereoselective glycosylations,[2,25−27] we recently identified a novel, scalable method to address many of the synthetic limitations previously associated with the construction of 1,2-cis-2-aminoglycosides (Scheme 1).[6,7,24,28−32] In our studies, we examined an array of glycosyl electrophiles and metal salts. From this evaluation, we discovered that the combination of C(2)-N-substituted trifluoromethylbenzylideneamino N-phenyl trifluoroacetimidate electrophiles **1** and nickel triflate, Ni(OTf)$_2$, provided high α-selectivity for 1,2-cis-amino linkage formation. However, some ambiguity about the mechanism and the catalyst still existed. Several reaction pathways have been proposed, including nickel directed glycosylation reaction, hydrogen-bond assisted reaction, glycosyl triflate promoted S$_N$2-like displacement, or imine addition followed by migration (vide infra, Figure 1).

The 1,2-cis-2-amino glycosylation reaction depicted in Scheme 1 involves a transfer of 15 mol % Ni(OTf)$_2$, generated in situ from nickel chloride (NiCl$_2$) and silver triflate (AgOTf), to a solution of N-phenyl trifluoroacetimidate **1** (1 equiv) and a glycosyl nucleophile (RO-H, 1.2 equiv) in methylene chloride at 25 °C. The reaction mixture is then allowed to proceed at 35 °C for 12 h to afford the 1,2-cis-2-amino product **2** in good yield and high diastereoselectivity. Ni(OTf)$_2$ is commercially available from several different sources and air-stable. However, we discovered that discrepancies did arise in the yield when different batches of Ni(OTf)$_2$ were used for the glycosylation.[24] In contrast, the in situ generation of Ni(OTf)$_2$, from NiCl$_2$ and AgOTf, resulted reproducible and consistent results.[24] From a practical point of view, it is worth noting that both NiCl$_2$ and AgOTf are commercially available, and they are not as deliquescent as other metal salts.[33] Therefore, in situ generated Ni(OTf)$_2$ became the catalyst of choice for the construction of several highly desired saccharide motifs containing 1,2-cis-2-amino linkages.[24,32]
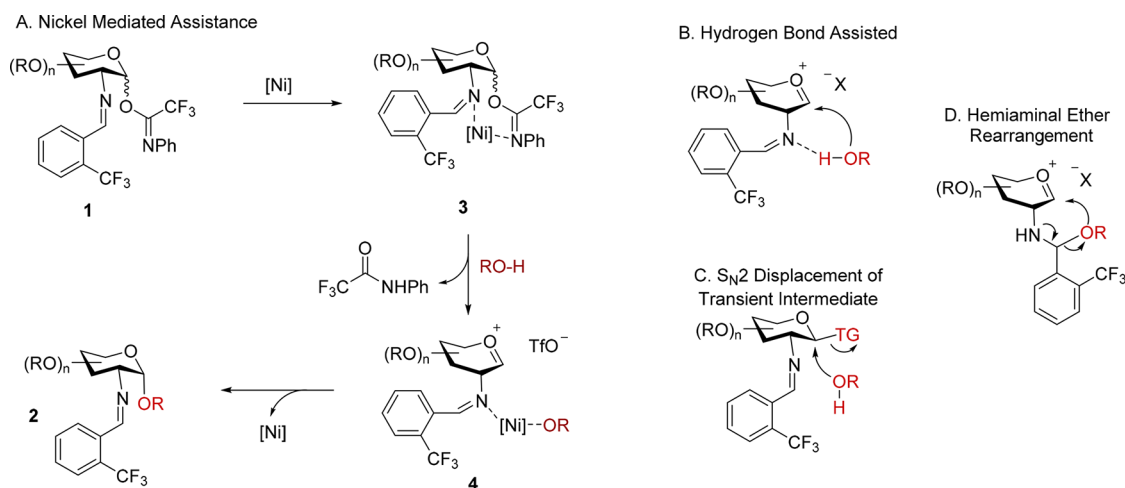

Figure 1. Potential reaction mechanisms for Ni(OTf)$_2$-catalyzed 1,2-cis-2-amino glycosylation.

Initial Mechanistic Investigations. Although a number of reaction pathways can be envisioned for the 1,2-*cis*-amino glycosylation, it is likely that the mechanism of the transformation proceeds via initial activation of the anomeric *N*-phenyl trifluoroacetimidate leaving group. In the original proposed mechanism, we hypothesize that Ni(OTf)$_2$ could effectively coordinate to both the benzylidene group at C(2) and the trifluoroacetimidate at C(1) of glycosyl electrophile **1** to form the corresponding nickel–substrate complex **3** (Figure 1a).[7] Subsequent ionization of **3** followed by exchange between the trifluoroacetamide group and the glycosyl nucleophile (RO-H) could generate a nickel–alkoxide complex **4**, which directs the addition of the alkoxide functionality to the *α*-face of an oxocarbenium intermediate to afford 1,2-*cis*-2-aminoglycoside **2**. Alternatively, one could invoke several other mechanistic pathways after imidate activation including S$_N$2 displacement of a temporary *β*-intermediate (Figure 1c). A second possibility is the addition of the acceptor to the *N*-benzylidene imine to form an unstable hemiaminal followed by migration to the *α*-face (Figure 1d). Lastly, the C(2)-imine could be utilized as a hydrogen-bond acceptor and assist in the delivery to the *α*-face (Figure 1b). Thus, our goal is to elucidate which mechanism is more likely to operate under Ni(OTf)$_2$-catalyzed glycosylation conditions.

Our first objective is to determine the role of Ni(OTf)$_2$ in the glycosylation or whether "hidden Brønsted acid catalysis" plays a role in the reaction. This is important because many reactions that utilize metal triflates (or a combination of metal halides and silver triflate) as catalysts are indeed activated by a Brønsted acid. In these reactions, traces of triflic acid (TfOH) which are slowly released from metal triflates are sufficient for the reaction to proceed.[9−14] As such, we hypothesized that triflic acid released from a combination of nickel chloride (NiCl$_2$) and silver triflate (AgOTf) could be responsible for the observed catalytic glycosylation as triflic acid has been used as a promoter of imidate glycosylation reactions.[34] To determine if triflic acid is the source of catalysis, glycosyl electrophile **5** and 1-adamantanol **6** were utilized as model coupling partners in our investigations to simplify the analysis of product mixtures (Table 1). In the experiment, the glycosylation of **6** with **5** was performed in the presence of 15 mol % *in situ* generated Ni(OTf)$_2$ and 60 mol % 2,6-di-*tert*-butyl-4-methylpyridine (DTBMP) as an acid scavenger (entry 2).[9] Consistent with our hypothesis, addition of DTBMP almost completely suppressed the reaction (less than 5% yield of the desired product **7** was detected), indicating that the reaction is activated by triflic acid.[21,22] Acid scavenger experiments typically are underutilized when metal triflates are the glycosylation catalyst.[35] In the absence of NiCl$_2$ or AgOTf, only a minuscule amount of **7** was observed (entries 3 and 4), and the coupling partners **5** and **6** were recovered quantitatively. These results establish that NiCl$_2$ and AgOTf serve as catalyst precursors for the *in situ* generation of Ni(OTf)$_2$, which then upon formation releases triflic acid.

Next, we explored the ability of other metal triflates to promote the 1,2-*cis*-2-amino glycosylation (Table 1, entries 5−7) to further validate whether triflic acid released from these metal salts is the source of catalysis. For metal salts with weakly coordinating anions, the release of Brønsted acids through cation hydrolysis has been documented.[36] In addition, there is a correlation between the catalytic activity of metal triflates and their hydrolysis constants (pK_h).[33] Cationic metals are generally difficult to hydrolyze when their pK_h values are
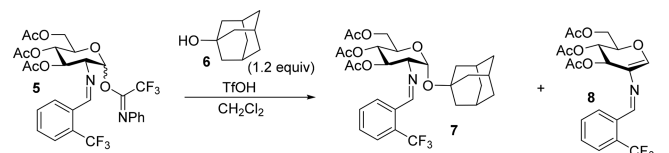
Table 1. Effect of Reaction Parameters

"standard" conditions
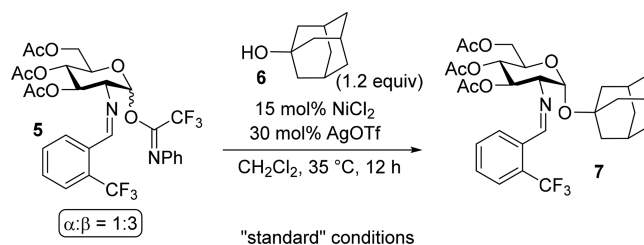
entry	variation from the "standard" conditions	yield[a] (%)	α:β ratio[b]
1	none	90	10:1
2	added 60 mol % DTBMP	5	n/a
3	no AgOTf	<1	n/a
4	no NiCl$_2$	6	n/a
5	1 equiv of AgOTf, instead of *in situ* generated Ni(OTf)$_2$	80	5:1
6	15 mol % Zn(OTf)$_2$, instead of *in situ* generated Ni(OTf)$_2$	91	10:1
7	15 mol % In(OTf)$_3$, instead of *in situ* generated Ni(OTf)$_2$	95	9:1
8	THF, instead of CH$_2$Cl$_2$	<1	n/a
9	EtCN, instead of CH$_2$Cl$_2$	<1	n/a
10	added 3 Å MS	<1	n/a

[a]Isolated yield. [b]Determined by ^{1}H NMR analysis.

greater than 10.1. In contrast, cations with pK_h values less than 4.3 are easy to hydrolyze.[33] For example, since the pK_h value of Ag(I) is too large (pK_h = 12) for hydrolysis to occur, almost no catalytic activity is observed in the glycosylation reaction, potentially from minimal release of triflic acid (entry 4, only 30 mol % AgOTf was utilized). The reaction proceeds to completion only in the presence of a stoichiometric amount of AgOTf (entry 5). In contrast, Ni(II) and Zn(II) have suitable pK_h values (9.86 for nickel and 8.96 for zinc), and thus their corresponding Ni(OTf)$_2$ and Zn(OTf)$_2$ sufficiently release triflic acid to catalyze the reaction and provide 1,2-*cis* glycoside **7** in excellent yield (entries 1 and 6). The easily hydrolyzable In(OTf)$_3$, whose pK_h value of In(III) is 4.0, was quite effective at catalyzing the reaction (entry 7). To compare, lanthanide triflates which are some of the most commonly used metal triflates for promoting glycosylation reactions have potential to go through a similar hydrolysis reaction as they have pK_h = ~7−8.[16] Furthermore, we hypothesize that the impact of Brønsted acid catalysis can be attenuated by employing Lewis basic solvents.[41] As expected, utilization of tetrahydrofuran (THF) or propionitrile (EtCN) completely suppresses the reaction (Table 1, entries 8 and 9). If Ni(OTf)$_2$ has been producing triflic acid species through hydrolytic interactions with adventitious H$_2$O, then molecular sieves will shut down the coupling event. We have found that no glycosidic bond (<1%) occurs with use of 3 Å activated molecular sieves (entry 10).[37] This result is consistent with our previous observation that utilization of commercially available Ni(OTf)$_2$ led to inconsistencies in the yield of the product when different batches were used.[24] These variances could arise from batch-to-batch variation of moisture content.[38]

It is well-documented that *in situ* generated triflic acid from metal triflates has distinct advantages over the direct use of triflic acid for several reasons: (i) Triflic acid is not readily soluble in apolar solvents, particularly in a small-scale experiments.[14] (ii) The use of triflic acid with equivalent amount to metal triflate in control experiments often can lead

Table 2. Effect of the Amount of Triflic Acid

| entry	TfOH loading (mol %)	temperature (°C)	reaction time (h)	conversion[a] (%)	7:8 ratio[a]	7 yield (%)[b]	7 α:β ratio[a]
1	10	25	1	100	3:1	73	10:1
2	5	25	3	85	11:1	78	10:1
3	1	25	24	35	>99:1	34	10:1
4	1	35	12	95	>99:1	78	10:1

[a]Determined by ^{1}H NMR analysis. [b]Isolated yield.

to the misleading impression that triflic acid is less effective than metal triflates due to product decomposition and significant amount of side products.[7,11] (iii) Triflic-acid-catalyzed control reactions often show inferior catalytic activity because they cannot receive the optimized amount of triflic acid that metal-triflate-catalyzed reactions generally receive. To validate these limitations, we probed the effect of varying amounts of triflic acid on the coupling efficiency (Table 2). These experiments also allowed us to compare qualitatively the rate of the glycosylation in the presence of triflic acid to that in the presence of nickel triflate. As illustrated in Table 2, although the reaction with use of 10 mol % TfOH proceeded to completion within 1 h at 25 °C (entry 1), a significant amount of elimination product **8** was observed (**7**:**8** = 3:1). Decreasing the triflic acid loading (entries 2 and 3) further suppressed formation of the side product **8**, but significantly slowed down the rate of glycosylation. Overall, these observations showed that the rate and the coupling efficiency catalyzed by 1 mol % TfOH at 35 °C (entry 4) was similar to that catalyzed by 15 mol % Ni(OTf)$_2$ at 35 °C (Table 1, entry 1).

At present, the nickel-triflate-catalyzed glycosylation protocol is conducted under acidic and elevated temperature conditions. Therefore, there is a possibility that postcoupling anomerization of the 1,2-*trans* glycosides to the thermodynamically stable 1,2-*cis* glycosides can occur.[39−48] As a result, we subjected an α- and β-mixture of product **7** to the standard glycosylation conditions catalyzed by either nickel triflate or triflic acid. No anomerization was observed after 12 h at 35 °C (Scheme 2). It appears that the α:β ratio of product **7** is kinetically derived and is not reflective of a thermodynamic distribution arising from postcoupling anomeric anomerization.

To understand how triflic acid is being produced from nickel triflate and acts as the active catalyst to promote the glycosylation, three control ^{19}F NMR experiments were conducted at 35 °C (Figure 2). Triflic acid was not detected from the reagent combination of NiCl$_2$ and AgOTf (Figure 2a)
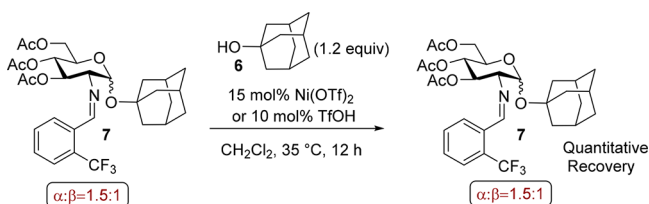
or from the mixture of NiCl$_2$, AgOTf, and an adamantanol nucleophile (Figure 2b). Interestingly, in the presence of glycosyl electrophile **5**, a broad singlet ^{19}F resonance at δ −78.99 ppm was detected (Figure 2c), a chemical shift which is consistent with characteristics of triflic acid (δ = −79.4 ± 0.5 ppm) (Figure S1).[14] Quantitative analysis of the newly formed broad singlet provides it at a 2 mol % ratio relative to **8** (Figure S1), which is nearly identical to the amount of triflic acid needed to replicate the results of the metal-triflate-catalyzed glycosylation (Table 2). This result suggests that residual moisture content of the carbohydrate substrate potentially facilitates the initial release of triflic acid from the metal center. Once the reaction initiated, triflic acid can be continuously generated through many other reaction pathways.

On the basis of the above observations, it is unlikely that nickel-coordinated delivery of an alkoxide nucleophile to generate 1,2-*cis*-2-amino product is the operative catalytic pathway (Figure 1a). *Importantly, these data further support that Brønsted acid catalysis is likely to operate in this reaction.* With the understanding that the reaction is catalyzed by "triflic acid" which is slowly released from Ni(OTf)$_2$, it is necessary to compare the benefits of both catalyst conditions. Although utilization of Ni(OTf)$_2$ does requires a two-step procedure, the precatalysts (NiCl$_2$ and AgOTf) used in the reaction are moisture-stable. In addition, slow release of triflic acid from Ni(OTf)$_2$ makes the method amenable to a wide variety of acid-sensitive protecting groups. On the other hand, use of pure triflic acid can quickly decompose acid-labile substrates; although the procedure is operationally simple, triflic acid is more moisture-sensitive leading to unpredictable yields when used at low catalytic loadings.

Next, we examined the role of triflic acid in influencing the stereochemical outcome of the glycosylation. Since the triflic acid released from Ni(OTf)$_2$ is the potential active catalyst, it is likely that a glycosyl triflate could be generated in the subsequent stages of the reaction.[23,49] The glycosyl triflate intermediate has been invoked to be involved in the formation of β-1,2-*cis*-mannoside products.[23,50−53] As a result, we hypothesize that substitution of Ni(OTf)$_2$ with nickel triflimide, Ni(NTf$_2$)$_2$, could impact the outcome of the selectivity.[51,54−58] Accordingly, the coupling of **6** with **5** was conducted in the presence of 15 mol % Ni(NTf$_2$)$_2$ (Scheme 3a), generated *in situ* from NiCl$_2$ and silver triflimide (AgNTf$_2$). Confirming our hypothesis, the reaction proceeded with poor anomeric stereoselectivity (α:β = 1.4:1). Similarly, use of triflimide, Tf$_2$NH (Scheme 3b), also provided a 1.3:1 mixture of α- and β-isomers. Lack of selectivity with use of the triflimide anion implies that the reaction goes through an
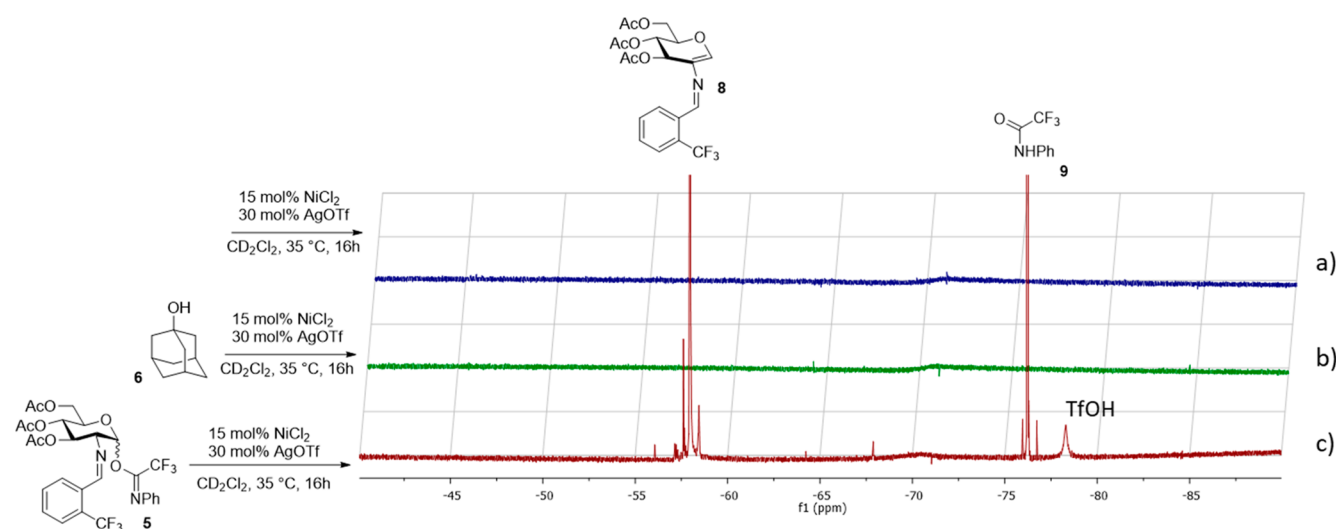
Scheme 2. Studies of Postcoupling Anomerization

Figure 2. Detection of triflic acid monitored at 35 °C by ^{19}F NMR in CD$_2$Cl$_2$: (a) Ni(OTf)$_2$ generated *in situ* from NiCl$_2$ and AgOTf; (b) adamantanol **6** and Ni(OTf)$_2$ generated *in situ* from NiCl$_2$ and AgOTf; (c) electrophile **5** and Ni(OTf)$_2$ generated *in situ* from NiCl$_2$ and AgOTf. Top portion of resonances corresponding to **8** and **9** has been removed; for full spectrum see Figure S1.

Scheme 3. Nickel-Triflimide-Catalyzed Glycosylation Reaction
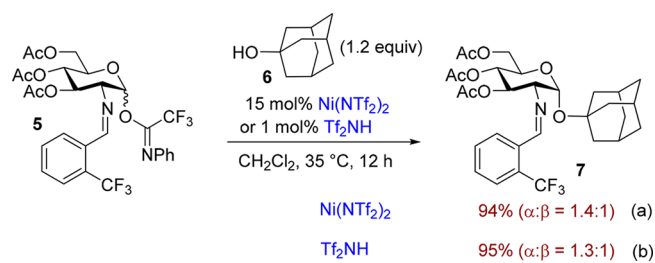
oxocarbenium ion intermediate in favor of an S$_N$1-type mechanism for the catalytic process. Furthermore, this observation suggests that both the hydrogen-bond assisted (Figure 1b) and hemiaminal rearrangement mechanisms (Figure 1d) are not likely to be the operational pathways. For both of the aforementioned pathways to be operative, the selectivity should remain the same regardless whether triflimide or triflate is used in the reaction. Overall, the poor selectivity observed with triflimide illustrates the importance of the triflate anion and further supports the possibility that the reaction goes through a transient glycosyl triflate intermediate.

Coinciding with the notion that the glycosyl triflate is the key intermediate in the reaction, we analyzed previously reported data in which we exchanged different substituents (both electron-donating and electron-withdrawing) on the C(2)-benzylidene group; there was no trend on the selectivity.[6] One would hypothesize that if an electron-donating substituent was placed on the aryl ring of the C(2)-benzylidene nitrogen which would become a better hydrogen-bond acceptor, higher α-selectivity could be observed (Pathway B, Figure 1). Alternatively, an electron-withdrawing substituent would increase the electrophilicity of the C(2)-benzylidene imine carbon, making nucleophile addition more favorable (Pathway D, Figure 1). Upon analysis, there was no correlation between the electronic nature of the substituent and the stereochemical outcome of the reaction. Thus, the data rule out that the proposed pathways B and D (Figure 1) are likely to be the operative pathways in the nickel-triflate-catalyzed glycosylation.

Finally, to further confirm that both anomers of *N*-phenyl trifluoroacetimidate **5** reacted to produce the 1,2-*cis*-2-amino
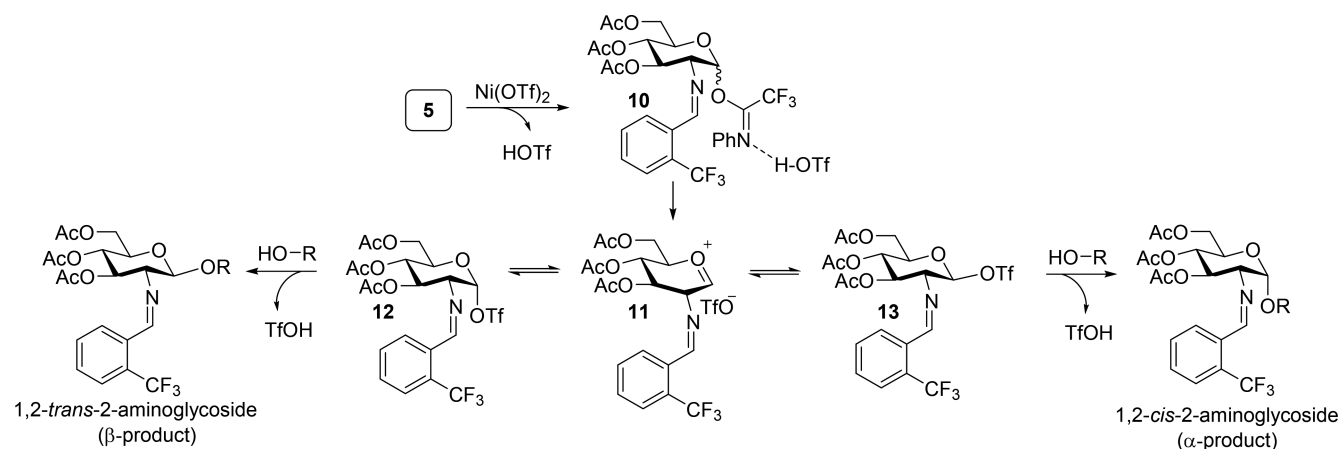

Figure 3. Proposed mechanism of triflic-acid-catalyzed glycosylation.
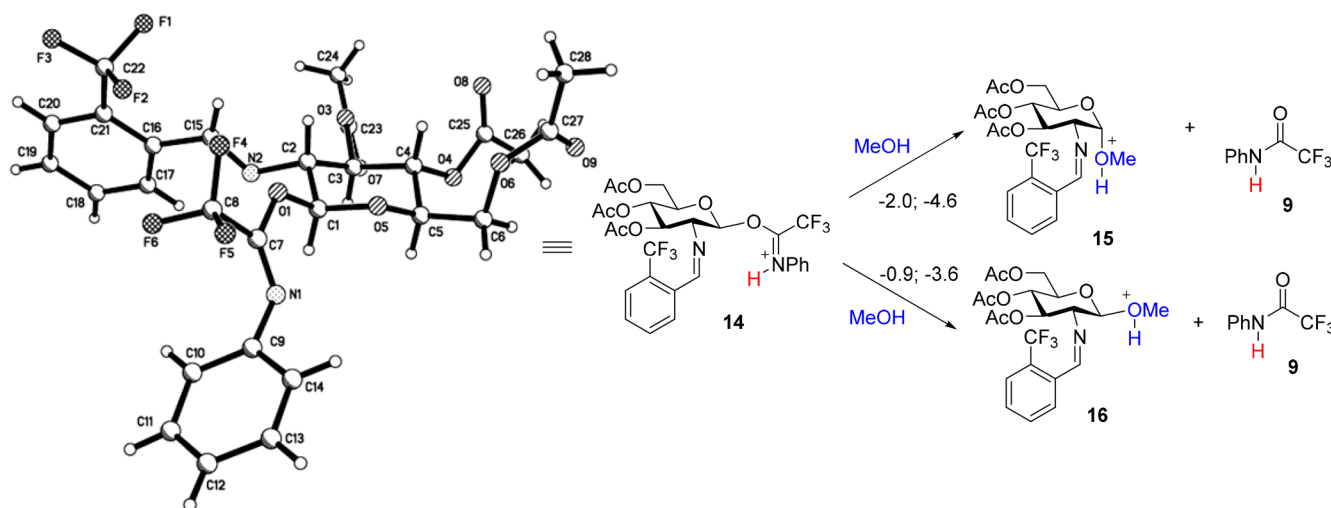
Figure 4. Overall reaction free energy for the formation of methyl glycosides. The initial computational model was formed from the crystal structure of the β-N-phenyl trifluoroacetimidate **5** (CCDC 1854007). Thermal ellipsoidal figure is included in the Supporting Information (Figure S21). Relative enthalpies (first number) and free energies (second number) are in kcal/mol (at 298 K) calculated using B3LYP/6-31G(d) with a SMD implicit solvent model.

product with similar selectivity, we separately subjected them to the 15 mol % $Ni(OTf)_2$ reaction conditions. While α-imidate **5** proceeded to completion within 4 h, β-imidate **5** progressed slowly and completed after 16 h. Nevertheless, they produced adamantanol glycoside **7** in α:β = 10:1 and similar yields (α, 95%; β, 88%). This result suggests that both anomers of imidate **5** are likely to proceed through the same reaction pathway.

Overall, our initial observations reveal several key aspects of the 1,2-cis-2-amino glycosylation. First, triflic acid released from nickel triflate is likely to be the active catalyst in effecting stereoselective formation of glycosidic bonds. Second, nickel triflate is not directly involved in the key glycosidic bond-forming process and serves as a precursor to the active triflic acid catalyst. Third, the presence of triflate anion is essential for the observed α-selectivity. Fourth, it is unlikely that the reaction proceeds through a nickel–substrate complex as we originally proposed (Figure 1a). An alternative pathway consistent with the aforementioned observations is illustrated in Figure 3. In the first step, TfOH, released from $Ni(OTf)_2$, can engage in electrophilic activation of the N-phenyl trifluoroacetimidate leaving group of glycosyl electrophile **5** to form the activated donor complex **10**. Subsequent ionization of **10** can lead to an array of reactive glycosyl intermediates. The oxocarbenium ion intermediate **11** can exist in a series of equilibria as it can be either closely associated with the triflate counterion in the form of contact ion pairs (CIPs) or further separated from the triflate counterion in the form of solvent separated ion pairs (SSIPs).[50] An intermediate such as **11** is likely as it can be obtained by both anomers of N-phenyl trifluoroacetimidate **5**, consistent with previous results that both α- and β-anomers provide the product with similar α-selectivity (α:β = 10:1). Triflic acid promoted stereoselective glycosylation via S_N1 pathway would have to bias the addition of a glycosyl nucleophile **6** to either diastereomeric face of this oxocarbenium ion-like intermediate **11** (Figure 3). Alternately, the two covalent glycosyl triflate intermediates **12** and **13** can be formed by nucleophilic attack of a triflate anion and are in equilibrium with oxocarbenium-like intermediate **11**.[51] Displacement of the covalent triflate species by a nucleophilic

partner takes place via an invertive S_N2 pathway, in such a way that the stereochemistry of the 2-aminosugar product would be dictated by the anomeric configuration of the glycosyl triflate intermediates. Although the glycosyl triflate has been reported to exist predominantly with an α-linkage (such as **12**) regardless of the electrophilic donor configuration, a dynamic system wherein α-glycosyl triflate is in equilibrium with its less stable but more reactive β-glycosyl triflate (such as **13**) has been proposed.[23,50,53] The rapid equilibrium between these two triflate anomers can take place at low temperatures (−78 °C).[23,50,53] Therefore, the equilibrium and the relative reactivity of the putative α- and β-covalent triflates could account for the observed selectivity in the formation of the 2-aminoglycoside products. This proposed catalytic glycosylation system, which affords 1,2-cis-2-aminoglycoside product **7** from the more reactive and less stable β-glycosyl triflate, is loosely reminiscent of a mechanism for 1,2-cis glycoside formation for α-glycosyl bromide in the presence of external bromide ion reported by Lemieux.[59]

Computational Investigation. To provide further insight into the reaction mechanism in which triflic acid plays a key role in controlling the 1,2-cis selectivity through rapid isomerization of transient glycosyl triflate intermediates followed by nucleophilic attack to the more reactive triflate species, we utilized density functional theory (DFT) calculations performed by the Gaussian program.[60] All geometries were optimized using the SMD[61] implicit solvent model and the B3LYP[62] functional with the 6-31G(d) basis set and corrected for basis set superposition error. Vibrational frequency calculations were used to confirm that the optimized structures are minima or transition state structures on the potential energy surface. To test the reliability of the B3LYP results, the single point energies for the B3LYP optimized geometries were also computed at the wB97XD/6-31+G(d) level of theory (Figure S22).[63] The potential energy surface computed at the wB97XD/6-31+G(d) level is consistent with the calculations at B3LYP/6-31G(d).

To benchmark our calculations, the proper orientation for the substituents in our computational model were determined from the crystal structure of the β-N-phenyl trifluoroacetimi-
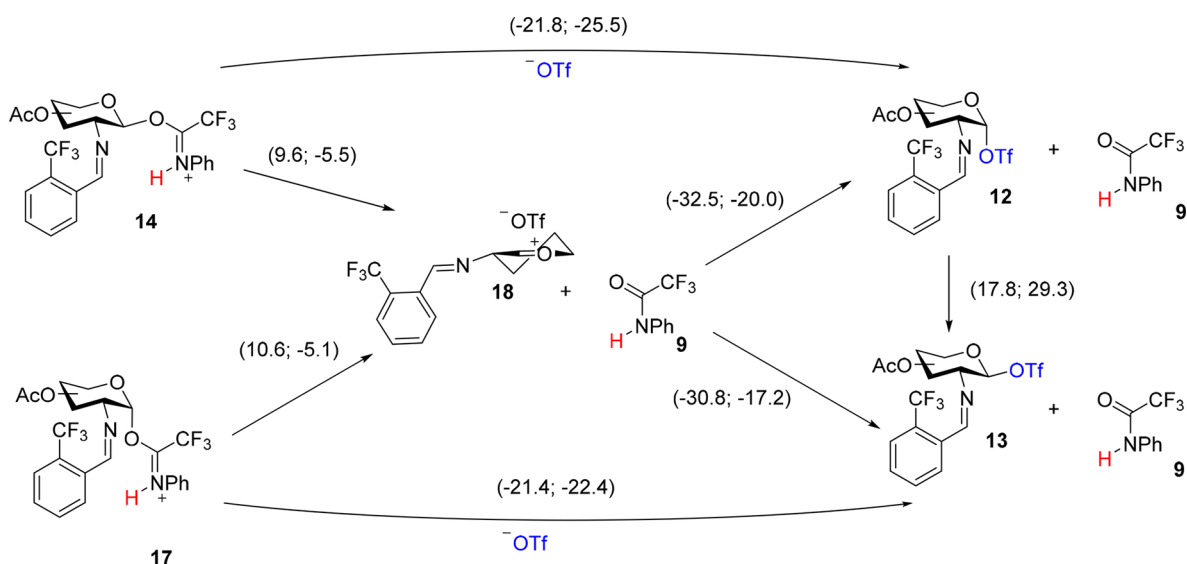
Figure 5. Energy of formation of glycosyl triflate intermediates **12** and **13**. Relative enthalpies (first number) and free energies (second number) are in kcal/mol (at 298 K).
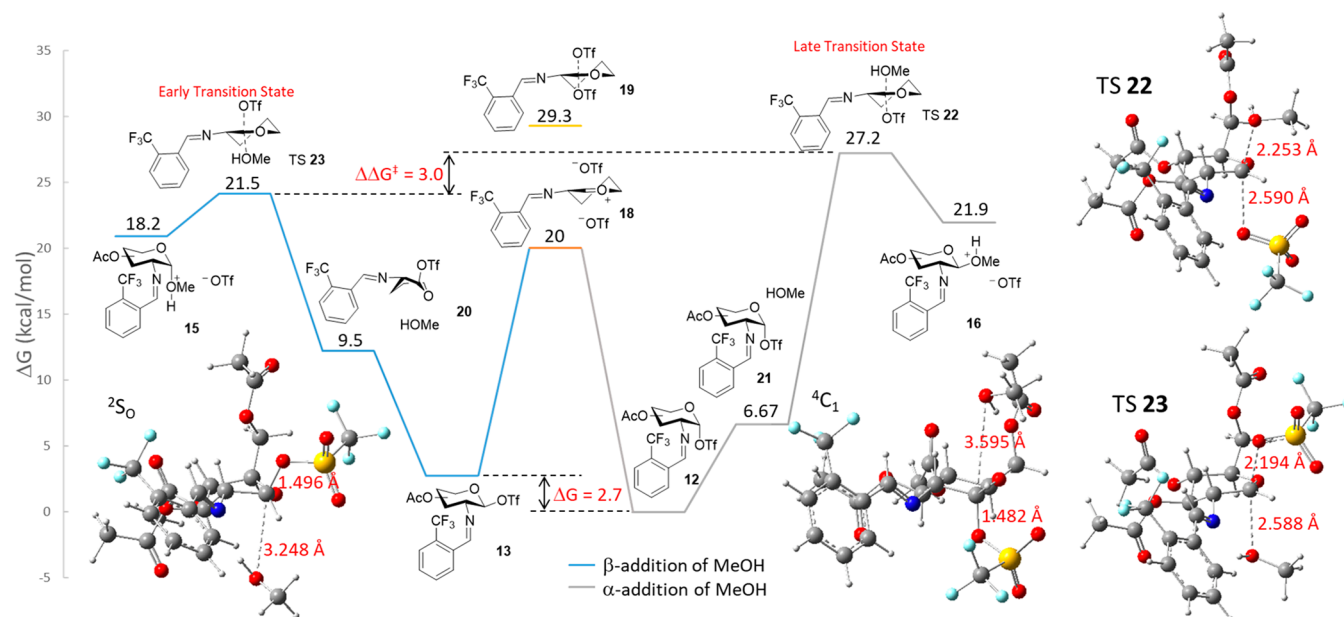

Figure 6. Energetic profile for the comparison of the isomerization of α-glycosyl triflate **12** to β-glycosyl triflate **13** versus their respective S_N2 displacements. Energies on the blue line are in respect to **13**, and energies on the gray line are in respect to **12** (units = kcal/mol).

date **5** (Figure 4 and Figure S21) which was obtained by a CH$_2$Cl$_2$/hexane slow diffusion at low temperature. We were able to confirm that the saccharide ring of the electrophile exists as a $^4C_1$ conformer, and the N-benzylidene prefers the E-configuration with the trifluoromethyl group positioned upward and in line with the imine group. From the derived structure, the initial computational study found the reaction free energies for the overall glycosylation involving protonated imidate **14** and methanol to be −4.6 and −3.6 kcal/mol, respectively, for the α- and β-methyl glycoside products (**15** and **16**, Figure 4). The formation of α- and β-methyl glycoside products is similar in reaction free energy, potentially rationalizing why a low $\alpha:\beta$ selectivity was obtained when the triflimide or nickel triflimide was used as the catalyst experimentally (Scheme 3). *This observation also implies that (a) there is the formation of an intermediate that plays a major*

role in controlling the product distribution, and (b) the selectivity does not come from a major inherent difference in the product energies.

To investigate the role of the glycosyl intermediate that enhances the 1,2-*cis* selectivity of the methyl glycoside product, a possible reaction pathway for the formation of α- and β-triflates (**12** and **13**, Figure 3) was examined. Upon protonation, the departure of the N-phenyl trifluoroacetimidate leads to formation of the contact oxocarbenium/triflate ion pair intermediate **18** (Figure 5) in the $^4H_3$ half-chair conformation by an exothermic process at −5.1 kcal/mol for the protonated α-imidate **17** and −5.5 kcal/mol for the protonated β-imidate **14** (for unprotonated data, see Figure S2). After the contact ion pair is formed, the oxocarbenium ion intermediate can produce either the α- and β-glycosyl triflates (**12** and **13**), both in an exothermic fashion (−20.0 and −17.2
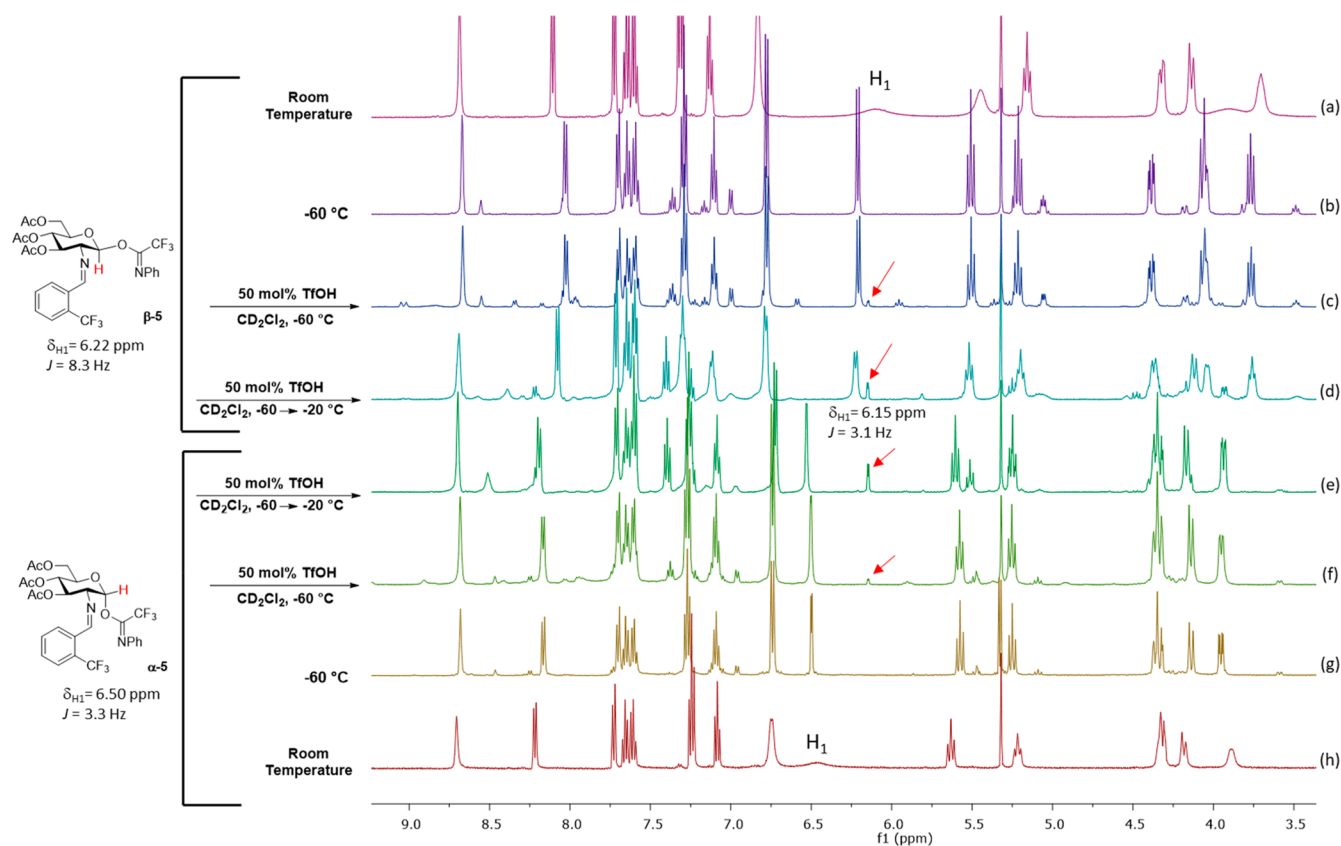
Figure 7. Addition of triflic acid to α- and β-imidates **5** was monitored by ^{1}H NMR in CD$_2$Cl$_2$: (a, h) α- and β-imidates **5** at room temperature; (b, g) α- and β-imidates **5** at −60 °C; (c, f) −60 °C, 20 min after addition of TfOH; and (d, e) −60 → −20 °C, 20 min.

kcal/mol). The large release in energy upon formation of the covalent triflates can be attributed to the electron-withdrawing nature of the *N*-benzylidene group destabilizing the oxocarbenium ion.[49,64] This observation is consistent with what has been observed with other short-lived transient intermediates (such as sulfonium ions) that direct stereoselectivity of the glycosylation.[65] Furthermore, electron-withdrawing protecting groups (such as acetyl groups) also provide stabilization of a covalent triflate avoiding the glycosylation to proceed via an oxocarbenium ion intermediate, but rather proceeding through an S$_N$2 displacement of a triflate.[65] We have previously observed that the S$_N$1−S$_N$2 glycosylation paradigm can be slightly shifted for C(2)-*N*-benzylidene imidates by replacement of the electron-withdrawing acetyl groups with the electron-donating benzyl groups (α only → 10:1).[29,31,54]

Calculations indicate that the α-glycosyl triflate is 2.8 kcal/mol more stable than β-glycosyl triflate (Figure 5).[46,47] Knowing that these anomers need to isomerize, we studied the conversion of α-triflate **12** to β-triflate **13** via a direct S$_N$2-like displacement with the triflate anion (TS**19**, Figure 6). However, the activation barrier for this direct substitution was calculated as 29.3 kcal/mol (Figure 5), suggesting that the preferred pathway for formation of β-glycosyl triflate **13** is the addition of the triflate anion to an oxocarbenium intermediate **18** in a CIP-type mechanism.

Following the calculations of the glycosyl triflate intermediates, the energy profile was calculated for the triflic-acid-mediated formation of 1,2-*cis*-2-aminoglycoside and is shown in Figure 6. When a methanol nucleophile is approaching the α-face of β-glycosyl triflate **13**, the methanol-β-triflate complex

intermediate begins to pucker into a ^2S_O conformation **20** ($d_{C(1)\text{-MeOH}}$ = 3.248 Å and $d_{C(1)\text{-OTf}}$ = 1.496 Å) with a change of 9.5 kcal/mol with respect to **13**. On the other hand, when a methanol nucleophile is approaching the opposite face of an α-glycosyl triflate **12**, the methanol-α-triflate complex intermediate maintains a $^4C_1$ conformation **21** ($d_{C(1)\text{-MeOH}}$ = 3.595 Å and $d_{C(1)\text{-OTf}}$ = 1.482 Å) with a barrier of 6.67 kcal/mol with respect to **12**. From **21**, nucleophilic attack of methanol to the β-face of α-triflate **12**, via transition state (TS**22**), requires an activation energy of 27.2 kcal/mol to form the β-protonated methyl glycoside **16**. Conversely, methanol attack to the α-face of β-triflate **13**, via TS**23**, requires an activation barrier of only 21.5 kcal/mol to form the α-protonated methyl glycoside **15**. Once the protonated glycoside product is generated, it will be quickly deprotonated to complete the catalytic cycle. Comparing two transition states (TS**22** and TS**23**), the energy difference (ΔΔG‡) is 3.0 kcal/mol in favor of the α-nucleophilic attack of methanol to the more reactive β-glycosyl triflate species. The Curtin−Hammett principle states that the product distribution can be influenced if anomerization of the α-triflate to the corresponding β-triflate intermediate is rapid and more favorable than the subsequent nucleophilic attack.[66] *Accordingly, the calculations for the product determining transition states have presented a higher activation barrier for nucleophilic attack to the opposite face of α-triflate (27.2 kcal/mol) in comparison to the anomerization of an α-triflate via an oxocarbenium ion to the β-triflate (20.0 kcal/mol) which is then followed by a quick subsequent nucleophilic attack to the opposite face (21.5 kcal/mol). These calculations are reflected in the experimental product distribution (vide infra, Figure 10) and support the proposed mechanism in Figure 3.*

We also performed a computational analysis to account for the reactivity differences between the two transition states, TS**22** and TS**23** (Figure S3). Looking at the optimized transition state structure of TS**23** for the α-nucleophile attack by methanol, the C−O bond length between the departing β-triflate group and the anomeric carbon is shorter than that between the incoming methanol and the anomeric carbon (2.194 Å vs 2.588 Å, Figure 6). A noncovalent interaction (NCI) plot was calculated for TS**23** (Figure S4), and no hydrogen-bonding interactions were found between the C(2)-imine nitrogen and the methanol molecule, further supporting that the stereoselectivity is not being derived from hydrogen bonding (see Figure 1b). The six-membered ring structure in TS**23** for the α-nucleophilic attack by methanol closely resembles the ^2S_O conformation of intermediate **20**, suggesting that the reaction proceeds through the early transition state. The puckered conformation of **20** is achieved to relieve potential steric interactions between methanol and the *N*-benzylidene in the transition state structure (TS**23**). According to the Hammond postulate, an early transition state (TS**23**) is preferred over a late transition state (TS**22**) as illustrated with the β-nucleophilic attack, wherein a six-membered ring remains in a productlike $^4C_1$ conformation as the nucleophile approaches.[67]

NMR Studies. With the possibility that the reaction goes through a transient triflate intermediate which is generated from the reaction of triflic acid with the glycosyl electrophile, we next attempted to detect this putative species spectroscopically. Although different types of glycosyl triflates have been observed by low-temperature NMR spectroscopy, there are few reports of α-triflate intermediates (**12**, Figure 3) generated from *N*-phenyl trifluoroacetimidate electrophiles.[49,68] As previously described by Yu, *N*-phenyl trifluoroacetimidate electrophiles present a unique challenge when monitoring by NMR.[69] These electrophiles are known to undergo inter-conversion via *syn*−*anti* isomerization around the carbon−nitrogen bond, resulting in a ¹H NMR spectrum with broad resonances.[69] As expected, both α- and β-imidates **5** were found at room temperature to have the broad anomeric proton resonances at δ 6.22 and 6.50, respectively (Figure 7a,h). However, at −60 °C interconversion is slow, and these anomeric proton resonances are no longer broad (Figure 7b,g). As a result, we could be able to confirm the anomeric configuration of both α- and β-imidates **5** (α-**5**, $^3J_{H1H2}$ = 3.3 Hz; β-**5**, $^3J_{H1H2}$ = 8.3 Hz) at −60 °C. The imine proton of the trifluoromethylbenzylidene group for both α- and β-imidates **5** appeared as a singlet resonance (δ 8.75) at room temperature (Figure 7a,h). Interestingly, we detected two sets of proton resonances (β-**5**, δ 8.75 and 8.65; α-**5**, δ 8.75 and 8.45) for these imine protons at −60 °C (Figure 7b,g), indicating that the *N*-phenyl group becomes locked in either the *E*- or *Z*-isomers at low temperature; however, the chemical environment around the imine proton is changed. To validate this proposal, a control study was performed in which each anomer in CD₂Cl₂ was cooled to −60 °C and gradually warmed to room temperature. Coalescence of these resonances into a single resonance δ 8.75 while taking the ¹H NMR spectra at different temperature intervals confirmed them as isomers (see Figures S5 and S6 in the SI).

Next, triflic acid (50 mol %) was added to the NMR tube containing β-imidate **5** at −60 °C (Figure 7c). Upon addition of TfOH, several new sets of proton resonances were detected, and there was a distinct doublet resonance resided at δ 9.0

ppm with a coupling constant value of 16.4 Hz. This downfield doublet resonance had corresponding integrations to two other resonances in the anomeric region, δ 6.60 (d, *J* = 8.4 Hz), δ 5.96 (t, *J* = 9.9 Hz). We established the identity of the proton resonance at δ 9.0 as a protonated iminium ion of β-imidate **5** by the addition of 50 mol % TfOH β-glycosyl acetate **S1** at −60 °C (Figure S7). The ¹H NMR spectrum of the corresponding protonated glycosyl acetate **S2** is illustrated in Figure S7, wherein the iminium proton resonance has a large *trans* coupling value of 15.4 Hz and resides at δ 9.03. The data is consistent with that of protonation of β-imidate **5**. The same findings were found for α-imidate **5**.

After identifying several proton resonances of the protonated α- and β-imidates **5**, our next goal is to determine the identity of the doublet resonance with a coupling constant value of 3.1 Hz at δ 6.15 (Figure 7). Consistent with our hypothesis that the reaction proceeds through the same intermediate, the resonance at δ 6.15 was detected in both α- and β-imidate **5** upon addition of TfOH (Figure 7c,f) at −60 °C. This also rules out anomerization of the imidate leaving group, as the anomeric resonance β-imidate was not detected in the spectrum of the α-counterpart and *vice versa*.[30] Since the chemical shift and coupling constant of this proton corresponds to the range of the previously reported anomeric proton resonance of α-glycosyl triflates (δ 6.0−6.5),[49] it was tentatively assigned as α-triflate **12** (Figure 3). A COSY 2D-NMR experiment of this putative glycosyl triflate intermediate indicated the resonance at δ 6.15 to be at the C(1) position (Figure S8a). Additionally, a HSQC 2D-NMR experiment of this presumed glycosyl triflate intermediate correlated the C(1) proton resonance at δ 6.15 to a ¹³C resonance of δ 105.62, which is analogous to the ¹³C resonance for the C(1) carbon of previously reported glycosyl triflates (Figure S8b).[49] Next, the reaction was allowed to gradually warm at 10 °C increments. At −20 °C, ¹H NMR spectral data contained only two major carbohydrate species which were identified as the unreacted imidate substrate **5** and the putative α-glycosyl triflate **12** (Figure 7d,e). Unfortunately, imidate **5** was not completely converted to the corresponding α-triflate **12** even in the presence of excess TfOH. Any further temperature increase above −20 °C led to decomposition into the highly conjugated glycal **8** and the undesired α-glycosyl acetate **26**. (*Vide infra*, Figure 10. Also see Figures S9 and S10 for VT-NMR decomposition experiments for α- and β-imidates **5**.)[70] To further verify the identity of the principal carbohydrate species as a glycosyl triflate, we conducted a control experiment using Tf₂NH in lieu of TfOH. We reasoned that if this species is the principal intermediate in the reaction, it would not be formed upon addition of Tf₂NH to α- and β-imidates **5**. Confirming our hypothesis, the proton resonance at δ 6.15 ppm was not observed for the reaction (see Figures S12 and S13 in the SI).

The subsequent stage in the glycosylation procedure involved the introduction of a nucleophile. We chose to use 2-propanol as a nucleophilic partner for ease of characterization of the carbohydrate intermediates. In the first scenario, 2-propanol (IPA) was introduced at the beginning of the reaction (Figure 8). A principal carbohydrate species having the proton resonance at δ 6.15 ppm was not detected. Upon warming of the reaction to 20 °C followed by quenching the mixture with triethylamine, formation of the isopropyl glycoside **24** was, however, observed with two doublet proton resonances (one at δ 4.96 ppm and other at δ 4.85 ppm) whose coupling constant values were 3.5 and 7.8 Hz,
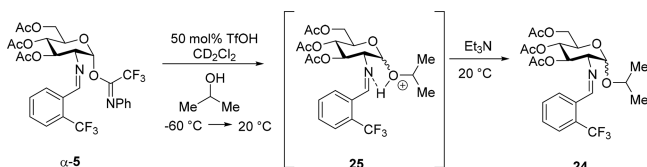
Figure 8. Glycosylation monitored by ^{1}H NMR in CD$_2$Cl$_2$.

respectively. This data suggests that the desired product **24** exists as a mixture of α- and β-isomers (Figure S14). As expected, **24** was isolated in 85% yield and 6:1 α:β selectivity, and no side products were detected. In comparison, when the glycosylation reaction was conducted in a Schlenk flask under nickel triflate conditions, a similar outcome was observed (78%, α:β = 8:1). It is worth noting that the ^{1}H NMR spectrum at 20 °C after full conversion did not look like that of the isolated isopropyl glycoside **24**. However, upon addition of triethylamine, the ^{1}H NMR spectrum became identical to the isolated product **24**, indicating that the protonated isopropyl glycoside **25** (Figure S14) was initially formed under acidic conditions. To validate that the principal carbohydrate species prior to triethylamine addition is simply the protonated glycoside **25**, the isolated product **24** was treated with 1 equiv of TfOH (see Figure S15) wherein the ^{1}H NMR spectrum matched that for the monitored NMR experiment. After quenching the reaction with triethylamine, the protonated glycoside product **25** was reverted to the isopropyl glycoside **24** with no change in α:β selectivity (Figure S15).

The complementary experiments were also performed by adding 2-propanol nucleophile after the putative glycosyl triflate with the proton resonance at δ 6.15 ppm was detected at −30 °C (**12**, Figure 9 and Figure S16). Upon gradual warming of the reaction at 10 °C increments, the desired glycoside **24** was detected along with other significant side products **8** and **26** (Figure 9). At the temperature range between −20 and −10 °C, an unexpected α-glycosyl acetate **26** (H$_1$ = δ 6.24, d, $^3J_{H1H2}$ = 3.2 Hz, Figure S16) was detected presumably via intermolecular acetyl migration. Formation of glycal **8** was also detected between −20 and −10 °C (Figure S16). At low temperatures, we hypothesize that the thermodynamically favored α-triflate has an increased population and could not rapidly undergo anomerization to the more reactive β-triflate. As a result of the increased pools of glycosyl triflate **12**, the elimination pathway to produce the conjugated glycal **8** is competing with the nucleophilic attack of 2-propanol to form the desired product **24**. On the other hand, under standard conditions at elevated temperature (35 °C), isomerization of the transient glycosyl triflate followed by nucleophilic attack occurs faster than the competing elimination pathway. As a result, glycal **8** was not detected when the reaction was conducted at 35 °C (Table 1, entry 1)
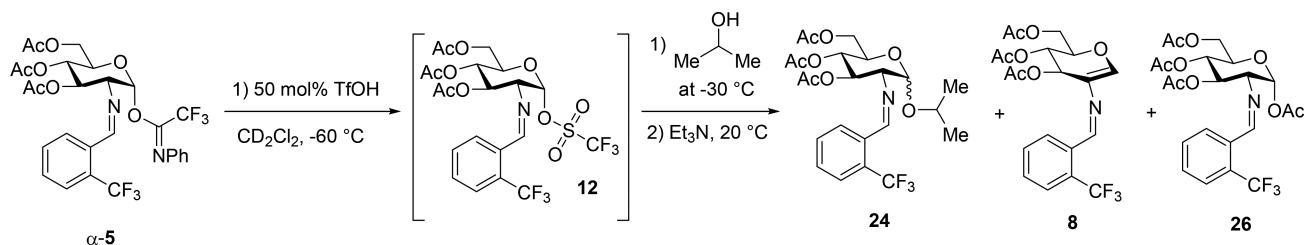
or when a nucleophile was introduced at the beginning of the reaction (Figure 8).

The need for interconversion from the α- to the β-glycosyl triflate intermediate (**12** and **13**, Figure 3) explains why we have observed selectivity changes with different glycosyl nucleophiles (Figure 10).[71] By using bulky or deactivated
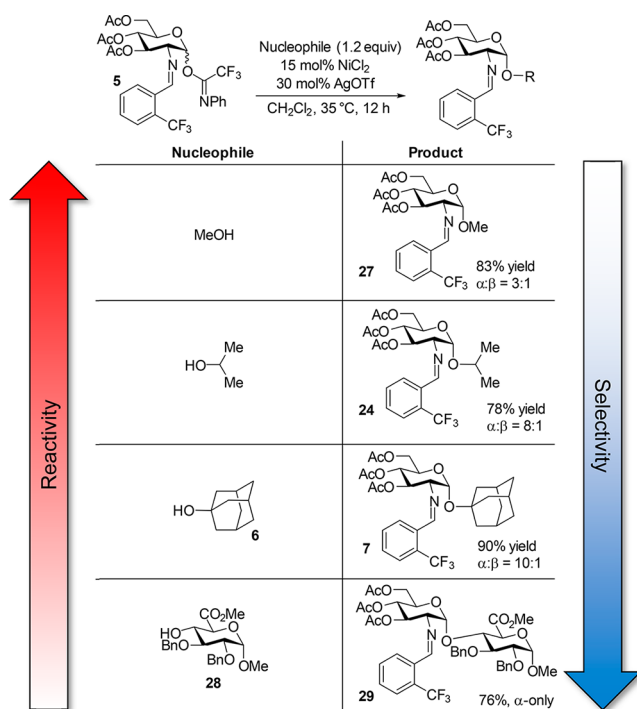

Figure 10. Relationship of reactivity of nucleophile and α:β selectivity of product under nickel-triflate-catalyzed conditions.

nucleophiles such as glucuronic acid **28** (α:β = 1:0)[24] and adamantanol **6** (α:β = 10:1), the reaction becomes very α-selective because more time is allowed for anomerization of the α-triflate to the more reactive β-triflate. An alternative explanation is that these acceptors are not reactive enough to displace the stable α-glycosyl triflate.[52,54,71−73] On the other hand, when a more reactive nucleophile is used in the reaction, the α-selectivity decreases significantly.[52,54,71−73] For instance, use of the highly reactive methanol provided the product **27** as a 3:1 α:β mixture, albeit in favor of α-anomer (for additional examples of acceptors, see ref 24).

It was also observed in a kinetics experiment that varying the equivalents of adamantanol **6** (Figure 11) had a significant impact on the selectivity of the reaction; however, there was no observed pattern for change in rate (Figure S17).[73] In contrast, there was a first order correlation when the amount of triflic acid catalyst was varied (Figure S18). For each different

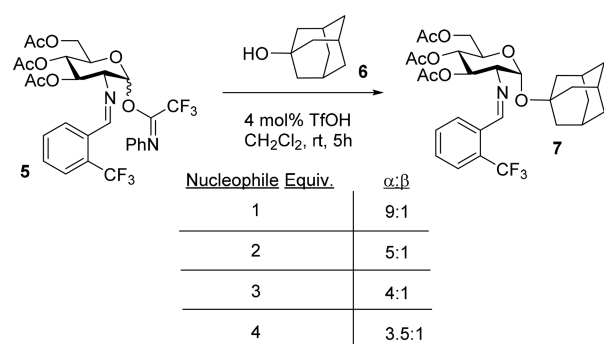**Figure 9.** Glycosylation monitored by ^{1}H NMR in CD$_2$Cl$_2$.

Figure 11. Kinetic study with different equivalents of nucleophile.

nucleophile concentration, the $\alpha:\beta$ selectivities were individually taken at multiple different time points. At a specific time point (5 h), increasing adamantanol **6** to 4 equiv dropped the $\alpha:\beta$ selectivity to 3.5:1, while only using 1 equiv of **6** produced the desired coupling product **7** in $\alpha:\beta$ = 9:1. We hypothesize that increasing the nucleophile concentration allows the nucleophilic attack to compete with the isomerization of α-glycosyl triflate to the corresponding β-glycosyl triflate, thus increasing the amount of β-product. Over the duration of the experiment, each nucleophile concentration showed an increase in $\alpha:\beta$ selectivity as time progressed because there is more time for the isomerization of the glycoysl triflate (Figure S17). These rate orders and changes in selectivity based on nucleophile concentration support a mechanism in which the rate is limited by the formation and isomerization of a glycosyl

triflate, that can then be facilely displaced by a nucleophile. Formation of the β-glycosyl triflate induces a bottleneck, making the nucleophile appear zeroth order.[73]

To further support the triflate isomerization hypothesis and to probe the influence of the C(2)-N-benzylidene on the formation of a glycosyl triflate intermediate, C(2)-azido- and C(2)-OBn-derived imidates were employed (**30** and **31**, Figure 12).[74−76] Upon subjection of 50 mol % TfOH at −50 °C, the previously reported C(2)-azido glycosyl α-triflate **32** was formed with a new anomeric resonance at δ 6.13 ppm (Figure S19 in the SI).[77] Upon warming the NMR probe, the C(2)-azido glycosyl triflate had a decomposition temperature of 0 °C, which is greater than that of the C(2)-N-benzylidene glycosyl triflate **12** (−20 °C). Alternatively, glycosyl triflate **33**, which was formed from subjecting C(2)-OBn imidate **31** to 50 mol % TfOH at −50 °C, decomposed at a slightly lower temperature of −30 °C (Figure S20). According to Crich and Codèe, a more stable α-glycosyl triflate does not allow for isomerization to the β-glycosyl triflate and will result in higher β-selectivity of the glycosylation product.[49,64,71] As expected, when the more electron-withdrawing C(2)-azido donor was subjected to a nickel-triflate-mediated coupling reaction with adamantanol **6**, the selectivity of the coupling product dropped to $\alpha:\beta$ = 4:1.[71] In contrast, the N-benzylidene and C(2)-benzyl ether modulate the electronics suitably allowing for the triflate to isomerize, thus resulting in higher α-selectivity (Figure 12).

An additional rationalization for the difference of these three imidates for high α-selectivity comes from the induction of an early transition state as the α-face attacking nucleophile interacts with the steric bulk of the N-benzylidene. On this
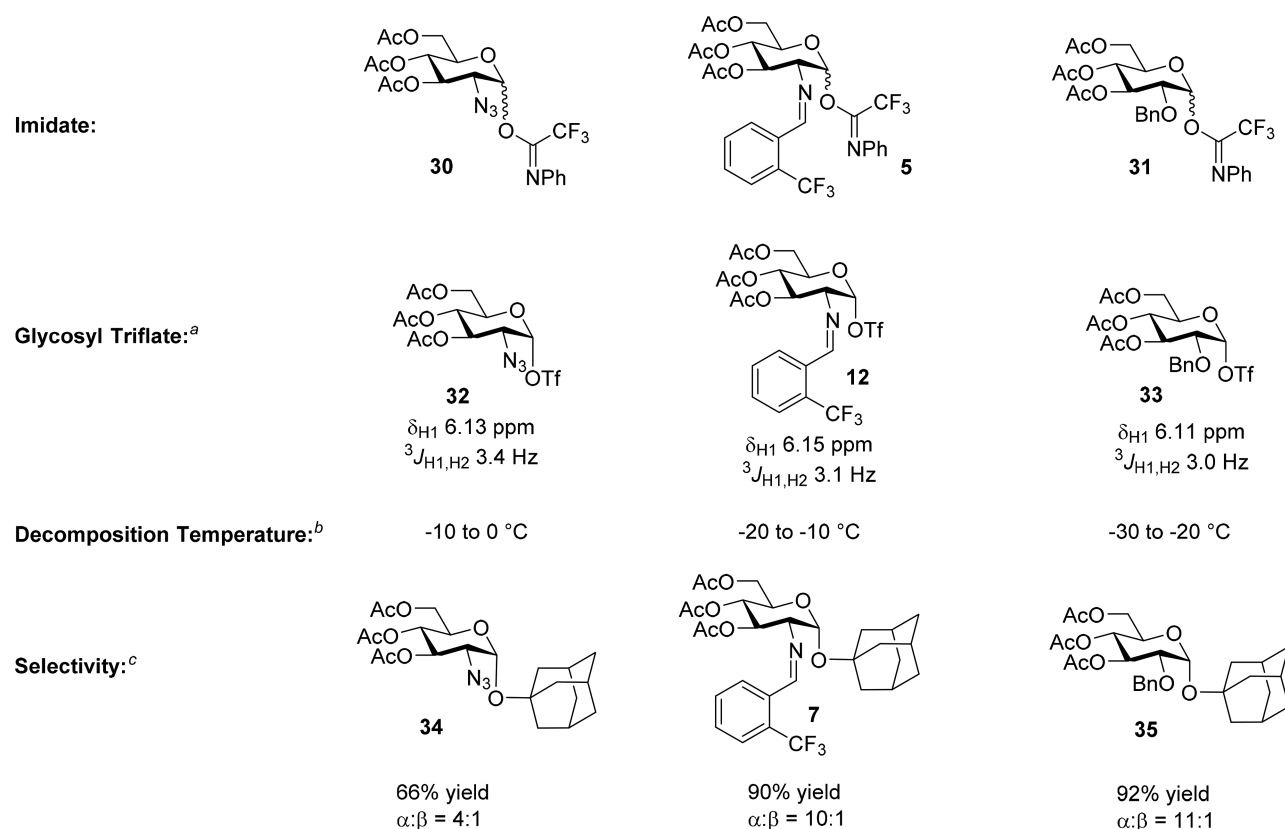

Figure 12. Relating the glycosyl triflate decomposition temperature to $\alpha:\beta$ selectivity of C(2)-protected glycosyl donors under Ni(OTf)$_2$-catalyzed conditions: (a) upon subjection of 50 mol % TfOH at −50 °C in CD$_2$Cl$_2$; (b) glycosyl triflate allowed to warm from −50 °C to room temperature while ^{1}H NMR was taken at 10 °C intervals; and (c) 15 mol % Ni(OTf)$_2$ in CH$_2$Cl$_2$.

basis, it has been reported that the *N*-benzylidene and *O*-benzyl protecting groups have similar size and can induce similar reactions because of their steric *A* value of 1.39,[78,79] whereas the azido group is smaller (steric *A* value = 0.45–0.62) and can perhaps not induce the early transition state as readily.[78,79]

CONCLUSIONS

In summary, we have presented the first systematic investigation of the release of triflic acid by a metal triflate for activation and its impact on the stereochemical outcome of metal-triflate-catalyzed glycosylation. As metal triflates are one of the most commonly utilized catalysts for glycosylations and provide many benefits over traditional activation methods, we have laid the foundation for future studies involving these catalysts as elucidations of their operative mechanism can be complex. We have shown that these catalysts are capable of producing triflic acid and that their hydrolysis constants should be taken into consideration. Once released, as systematically studied in our nickel-triflate-catalyzed glycosylation mechanism, triflic acid can influence the anomeric selectivity through a generation of a transient glycosyl triflate. However, a glycosyl triflate mechanism is not universal in affecting the selectivity of the newly formed glycosidic bond; a multitude of other factors need to be taken into consideration when trying to rationalize selectivity, including protecting groups and carbohydrate coupling partners. Under our nickel-triflate-catalyzed conditions, the release of triflic acid in combination with the unique stereoelectronic nature of the C(2)-*N*-benzylidene group on glycosyl *N*-phenyl trifluoroacetimidate provided the formation of 1,2-*cis*-aminoglycosides to be highly favorable.

ASSOCIATED CONTENT

Ⓢ Supporting Information

The Supporting Information is available free of charge on the ACS Publications website at DOI: 10.1021/acscatal.8b04444.

> Full experimental procedures and characterization data for all new compounds (PDF)
>
> X-ray data for compound *β*-imidate **5** (CIF)

AUTHOR INFORMATION

Corresponding Authors
*E-mail: hbs@chem.wayne.edu.
*E-mail: hien.nguyen@chem.wayne.edu.
ORCID ⊙
Yi-Jung Tu: 0000-0003-4114-6105
H. Bernhard Schlegel: 0000-0001-7114-2821
Hien M. Nguyen: 0000-0002-7626-8439
Notes
The authors declare no competing financial interest.

ACKNOWLEDGMENTS

REFERENCES

(1) Varki, A. Biological Roles of Oligosaccharides: All of the Theories are Correct. *Glycobiology* **1993**, *3*, 97−130.

(2) McKay, M. J.; Nguyen, H. M. Recent Advances in Transition Metal-Catalyzed Glycosylation. *ACS Catal.* **2012**, *2*, 1563−1595.

(3) Li, X.; Zhu, J. Glycosylation via Transition-Metal Catalysis: Challenges and Opportunities. *Eur. J. Org. Chem.* **2016**, *2016*, 4724−4767.

(4) Nielsen, M. M.; Pedersen, C. M. Catalytic Glycosylations in Oligosaccharide Synthesis. *Chem. Rev.* **2018**, *118*, 8285−8358.

(5) Zhu, Y.; Yu, B. Highly Stereoselective *β*-Mannopyranosylation via the 1-*α*-Glycosyloxy-isochromenylium-4-gold(I) Intermediates. *Chem. - Eur. J.* **2015**, *21*, 8771−8780.

(6) Mensah, E. A.; Yu, F.; Nguyen, H. M. Nickel-Catalyzed Stereoselective Glycosylation with C(2)-N-Substituted Benzylidene D-Glucosamine and Galactosamine Trichloroacetimidates for the Formation of 1,2-Cis-2-Amino Glycosides. Applications to the Synthesis of Heparin Disaccharides, GPI Anchor Pseudodisaccharides, and Alpha-GalNAc. *J. Am. Chem. Soc.* **2010**, *132*, 14288−14302.

(7) Mensah, E. A.; Nguyen, H. M. Nickel-Catalyzed Stereoselective Formation of Alpha-2-Deoxy-2-Amino Glycosides. *J. Am. Chem. Soc.* **2009**, *131*, 8778−8780.

(8) Zhu, X.; Schmidt, R. R. New Principles for Glycoside-Bond Formation. *Angew. Chem., Int. Ed.* **2009**, *48*, 1900−1934.

(9) Wabnitz, T. C.; Yu, J.-Q.; Spencer, J. B. Evidence That Protons Can Be the Active Catalysts in Lewis Acid Mediated Hetero-Michael Addition Reactions. *Chem. - Eur. J.* **2004**, *10*, 484−493.

(10) Li, Z.; Zhang, J.; Brouwer, C.; Yang, C.-G.; Reich, N. W.; He, C. Brønsted Acid Catalyzed Addition of Phenols, Carboxylic Acids, and Tosylamides to Simple Olefins. *Org. Lett.* **2006**, *8*, 4175−4178.

(11) Rosenfeld, D. C.; Shekhar, S.; Takemiya, A.; Utsunomiya, M.; Hartwig, J. F. Hydroamination and Hydroalkoxylation Catalyzed by Triflic Acid. Parallels to Reactions Initiated with Metal Triflates. *Org. Lett.* **2006**, *8*, 4179−4182.

(12) Taylor, J. G.; Adrio, L. A.; Hii, K. K. Hydroamination Reactions by Metal Triflates: Brønsted Acid vs. Metal Catalysis? *Dalton Trans* **2010**, *39*, 1171−1175.

(13) McKinney Brooner, R. E.; Widenhoefer, R. A. Stereochemistry and Mechanism of the Brønsted Acid Catalyzed Intramolecular Hydrofunctionalization of an Unactivated Cyclic Alkene. *Chem. - Eur. J.* **2011**, *17*, 6170−6178.

(14) Dang, T. T.; Boeck, F.; Hintermann, L. Hidden Brønsted Acid Catalysis: Pathways of Accidental or Deliberate Generation of Triflic Acid from Metal Triflates. *J. Org. Chem.* **2011**, *76*, 9353−9361.

(15) Crasto, C. F.; Jones, G. B. A Practical method for preparation of *β*-glycosides of N-acetylglucosamine. *Tetrahedron Lett.* **2004**, *45*, 4891−4894.

(16) Sanders, W. J.; Kiessling, L. L. Stereoselective, Lewis Acid-Catalyzed Glycosylation of Alcohols by Glucose 1,2-Cyclic Sulfites. *Tetrahedron Lett.* **1994**, *35*, 7335−7338.

(17) Kristensen, S. K.; Salamone, S.; Rasmussen, M. R.; Marqvorsen, M. H. S.; Jensen, H. H. Glycosyl ortho-Methoxybenzoates: Catalytically Activated Glycosyl Donors with an Easily Removable and Recyclable Leaving Group. *Eur. J. Org. Chem.* **2016**, *2016*, 5365−5376.

(18) Adinolfi, M.; Barone, G.; Iadonisi, A.; Schiattarella, M. Efficient Activation of Glycosyl N-(Phenyl)trifluoroacetimidate Donors with Ytterbium(III) Triflate in the Glycosylation Reaction. *Tetrahedron Lett.* **2002**, *43*, 5573−5577.

(19) Christensen, H.; Christiansen, M. S.; Petersen, J.; Jensen, H. H. Direct Formation of *β*-Glycosides of N-Acetyl Glycosamines Mediated by Rare Earth Metal Triflates. *Org. Biomol. Chem.* **2008**, *6*, 3276−3283.

(20) Rasmussen, M. R.; Marqvorsen, M. H. S.; Kristensen, S. K.; Jensen, H. H. A Protocol for Metal Triflate Catalyzed Direct Glycosylations with GalNAc 1-OPiv Donors. *J. Org. Chem.* **2014**, *79*, 11011−11019.

(21) Dumeunier, R.; Markó, I. E. On the Role of Triflic Acid in the Metal Triflate-Catalysed Acylation of Alcohols. *Tetrahedron Lett.* **2004**, *45*, 825−829.

(22) Bizier, N. P.; Atkins, S. R.; Helland, L. C.; Colvin, S. F.; Twitchell, J. R.; Cloninger, M. J. Indium Triflate Catalyzed Peracetylation of Carbohydrates. *Carbohydr. Res.* **2008**, *343*, 1814−1818.

(23) Crich, D.; Sun, S. Are Glycosyl Triflates Intermediates in the Sulfoxide Glycosylation Method? A Chemical and 1H, 13C, and 19F NMR Spectroscopic Investigation. *J. Am. Chem. Soc.* **1997**, *119*, 11217−11223.

(24) Sletten, E. T.; Ramadugu, S. K.; Nguyen, H. M. Utilization of Bench-Stable and Readily Available Nickel(II) Triflate for Access to 1,2-Cis-2-Aminoglycosides. *Carbohydr. Res.* **2016**, *435*, 195−207.

(25) Yang, J.; Cooper-Vanosdell, C.; Mensah, E. A.; Nguyen, H. M. Cationic Palladium-Catalyzed Stereoselective Glycosylation with Glycosyl Trichloroacetimidates. *J. Org. Chem.* **2008**, *73*, 794−800.

(26) Mensah, E. A.; Azzarelli, J. M.; Nguyen, H. M. Palladium-Controlled Beta-Selective Glycosylation in the Absence of the C(2)-Ester Participatory Group. *J. Org. Chem.* **2009**, *74*, 1650−1657.

(27) McKay, M. J.; Naab, B. D.; Mercer, G. J.; Nguyen, H. M. Selective Formation of Beta-O-Aryl Glycosides in the Absence of the C(2)-Ester Neighboring Group. *J. Org. Chem.* **2009**, *74*, 4705−4711.

(28) Yu, F.; Nguyen, H. M. Studies on the Selectivity Between Nickel-Catalyzed 1,2-Cis-2-Amino Glycosylation of Hydroxyl Groups of Thioglycoside Acceptors with C2-Substituted Benzylidene N-Phenyl Trifluoroacetimidates and Intermolecular Aglycon Transfer of the Sulfide Group. *J. Org. Chem.* **2012**, *77*, 7330−7343.

(29) McConnell, M. S.; Yu, F.; Nguyen, H. M. Nickel-Catalyzed Alpha-Glycosylation of C(1)-Hydroxyl D-Myo-Inositol: A Formal Synthesis of Mycothiol. *Chem. Commun.* **2013**, *49*, 4313−4315.

(30) McConnell, M. S.; Mensah, E. A.; Nguyen, H. M. Stereoselective Alpha-Glycosylation of C(6)-Hydroxyl Myo-Inositols via Nickel Catalysis-Application to the Synthesis of GPI Anchor Pseudo-Oligosaccharides. *Carbohydr. Res.* **2013**, *381*, 146−152.

(31) Yu, F.; McConnell, M. S.; Nguyen, H. M. Scalable Synthesis of Fmoc-Protected GalNAc-Threonine Amino Acid and Tn Antigen via Nickel Catalysis. *Org. Lett.* **2015**, *17*, 2018−2021.

(32) Bennett, C. S. *Selective Glycosylations Synthetic Methods and Catalysts*; Wiley-VCH: Weinheim, Germany, 2017; pp 1−378.

(33) Kobayashi, S.; Nagayama, S.; Busujima, T. Lewis Acid Catalysts Stable in Water. Correlation between Catalytic Activity in Water and Hydrolysis Constants and Exchange Rate Constants for Substitution of Inner-Sphere Water Ligands. *J. Am. Chem. Soc.* **1998**, *120*, 8287−8288.

(34) Glibstrup, E.; Pedersen, C. M. Scalable Synthesis of Anomerically Pure Orthogonal-Protected GlcN3 and GalN3 from d-Glucosamine. *Org. Lett.* **2016**, *18*, 4424−4427.

(35) There are several examples in the literature in which the reaction still proceeding when an acid scavenger was used in the presence of a metal triflate. Medina, S.; Henderson, A. S.; Bower, J. F.; Galan, M. C. *Chem. Commun.* **2015**, *51*, 8939−8941.

(36) Baes, C. F.; Mesmer, R. E. *The Hydrolysis of Cations*; Wiley: New York, 1976; XXI, p. 489.

(37) Similar triflic acid promoted reactions have been known to proceed in the presence of molecular sieves: Despras, G.; Urban, D.; Vauzeilles, B.; Beau, J.-M. *Chem. Commun.* **2014**, *50*, 1067.

(38) Godeau, J.; Fontaine-Vive, F.; Antoniotti, S.; Duñach, E. Experimental and Theoretical Studies on the Bismuth-Triflate-Catalysed Cycloisomerisation of 1,6,10-Trienes and Aryl Polyenes. *Chem. - Eur. J.* **2012**, *18*, 16815−16822.

(39) Lemieux, R. U.; Shyluk, W. P.; Huber, G. The Acetolyses of the Alpha and Beta-Methyl D-Glucopyranoside Tetraacetates. *Can. J. Chem.* **1955**, *33*, 148−162.

(40) Normant, J. F.; Alexakis, A.; Ghribi, A.; Mangeney, P. Boron Fluoride Promoted Cleavage of Acetals by Organocopper Reagents Application to Asymmetric Synthesis. *Tetrahedron* **1989**, *45*, 507−516.

(41) Ikemoto, N.; Kim, O. K.; Lo, L.-C.; Satyanarayana, V.; Chang, M.; Nakanishi, K. Ferric Chloride, an Anomerization Aatalyst for the Preparation of Alkyl α-Glycopyranosides. *Tetrahedron Lett.* **1992**, *33*, 4295−4298.

(42) Olsson, R.; Rundström, P.; Persson, B.; Frejd, T. Organo-titanium-Induced Stereoselective Alkylative Endo-Cleavage of Benzyl Pentopyranosides. *Carbohydr. Res.* **1998**, *307*, 13−18.

(43) O'Brien, C.; Poláková, M.; Pitt, N.; Tosin, M.; Murphy, P. V. Glycosidation−Anomerisation Reactions of 6,1-Anhydroglucopyranuronic Acid and Anomerisation of β-D-Glucopyranosiduronic Acids Promoted by SnCl4. *Chem. - Eur. J.* **2007**, *13*, 902−909.

(44) Wang, Y.; Cheon, H.-S.; Kishi, Y. Unique Reactivity of the Mukaiyama Glycosidation Catalyst (SnCl3ClO4) Toward β-Mannopyranosides. *Chem. - Asian J.* **2008**, *3*, 319−326.

(45) Pilgrim, W.; Murphy, P. V. SnCl4- and TiCl4-Catalyzed Anomerization of Acylated O- and S-Glycosides: Analysis of Factors That Lead to Higher α:β Anomer Ratios and Reaction Rates. *J. Org. Chem.* **2010**, *75*, 6747−6755.

(46) Manabe, S.; Satoh, H.; Hutter, J.; Lüthi, H. P.; Laino, T.; Ito, Y. Significant Substituent Effect on the Anomerization of Pyranosides: Mechanism of Anomerization and Synthesis of a 1,2-cis Glucosamine Oligomer from the 1,2-trans Anomer. *Chem. - Eur. J.* **2014**, *20*, 124−132.

(47) Satoh, H.; Manabe, S.; Ito, Y.; Lüthi, H. P.; Laino, T.; Hutter, J. Endocyclic Cleavage in Glycosides with 2,3-trans Cyclic Protecting Groups. *J. Am. Chem. Soc.* **2011**, *133*, 5610−5619.

(48) Vidadala, S. R.; Pimpalpalle, T. M.; Linker, T.; Hotha, S. Gold-Catalyzed Reactions of 2-C-Branched Carbohydrates: Mild Glycosidations and Selective Anomerizations. *Eur. J. Org. Chem.* **2011**, *2011*, 2426−2430.

(49) Frihed, T. G.; Bols, M.; Pedersen, C. M. Mechanisms of Glycosylation Reactions Studied by Low-Temperature Nuclear Magnetic Resonance. *Chem. Rev.* **2015**, *115*, 4963−5013.

(50) Huang, M.; Garrett, G. E.; Birlirakis, N.; Bohe, L.; Pratt, D. A.; Crich, D. Dissecting the Mechanisms of a Class of Chemical Glycosylation using Primary 13C Kinetic Isotope Effects. *Nat. Chem.* **2012**, *4*, 663−667.

(51) Dhakal, B.; Bohe, L.; Crich, D. Trifluoromethanesulfonate Anion as Nucleophile in Organic Chemistry. *J. Org. Chem.* **2017**, *82*, 9263−9269.

(52) van der Vorm, S.; Hansen, T.; Overkleeft, H. S.; van der Marel, G. A.; Codée, J. D. C. The Influence of Acceptor Nucleophilicity on the Glycosylation Reaction Mechanism. *Chem. Sci.* **2017**, *8*, 1867−1875.

(53) Crich, D.; Cai, W. Chemistry of 4,6-O-Benzylidene-D-glycopyranosyl Triflates: Contrasting Behavior between the Gluco and Manno Series. *J. Org. Chem.* **1999**, *64*, 4926−4930.

(54) Adero, P. O.; Amarasekara, H.; Wen, P.; Bohe, L.; Crich, D. The Experimental Evidence in Support of Glycosylation Mechanisms at the SN1-SN2 Interface. *Chem. Rev.* **2018**, *118*, 8242−8284.

(55) Kowalska, K.; Pedersen, C. M. Catalytic Stereospecific O-Glycosylation. *Chem. Commun.* **2017**, *53*, 2040−2043.

(56) Qiao, Y.; Ge, W.; Jia, L.; Hou, X.; Wang, Y.; Pedersen, C. M. Glycosylation intermediates studied using low temperature 1H- and 19F-DOSY NMR: new insight into the activation of trichloroacetimidates. *Chem. Commun.* **2016**, *52*, 11418−11421.

(57) Zandanel, C.; Dehuyser, L.; Wagner, A.; Baati, R. Highly Chemo- and Stereoselective Glycosidation of Permethacrylated O-Glycosyl Trichloroacetimidate Reagents Promoted by TMSNTf2. *Tetrahedron* **2010**, *66*, 3365−3369.

(58) Elferink, H.; Pedersen, C. M. l-Rhamnosylation: The Solvent is the Solution. *Eur. J. Org. Chem.* **2017**, *2017*, 53−59.

(59) Lemieux, R. U.; Hendriks, K. B.; Stick, R. V.; James, K. Halide Ion Catalyzed Glycosidation Reactions. Syntheses of alpha-Linked Disaccharides. *J. Am. Chem. Soc.* **1975**, *97*, 4056−4062.

(60) Frisch, M. J.; Trucks, G. W.; Schlegel, H. B.; Scuseria, G. E.; Robb, M. A.; Cheeseman, J. R.; Scalmani, G.; Barone, V.; Mennucci, B.; Petersson, G. A.; Nakatsuji, H.; Caricato, M.; Li, X.; Hratchian, H. P.; Izmaylov, A. F.; Bloino, J.; Zheng, G.; Sonnenberg, J. L.; Hada, M.;

Ehara, M.; Toyota, K.; Fukuda, R.; Hasegawa, J.; Ishida, M.; Nakajima, T.; Honda, Y.; Kitao, O.; Nakai, H.; Vreven, T.; Montgomery, J. A., Jr.; Peralta, J. E.; Ogliaro, F.; Bearpark, M.; Heyd, J. J.; Brothers, E.; Kudin, K. N.; Staroverov, V. N.; Kobayashi, R.; Normand, J.; Raghavachari, K.; Rendell, A.; Burant, J. C.; Iyengar, S. S.; Tomasi, J.; Cossi, M.; Rega, N.; Millam, J. M.; Klene, M.; Knox, J. E.; Cross, J. B.; Bakken, V.; Adamo, C.; Jaramillo, J.; Gomperts, R.; Stratmann, R. E.; Yazyev, O.; Austin, A. J.; Cammi, R.; Pomelli, C.; Ochterski, J. W.; Martin, R. L.; Morokuma, K.; Zakrzewski, V. G.; Voth, G. A.; Salvador, P.; Dannenberg, J. J.; Dapprich, S.; Daniels, A. D.; Farkas, O.; Foresman, J. B.; Ortiz, J. V.; Cioslowski, J.; Fox, D. J. *Gaussian 09*, revision D.01; Gaussian, Inc.: Wallingford, CT, 2009.

(61) Marenich, A. V.; Cramer, C. J.; Truhlar, D. G. Universal Solvation Model Based on Solute Electron Density and on a Continuum Model of the Solvent Defined by the Bulk Dielectric Constant and Atomic Surface Tensions. *J. Phys. Chem. B* **2009**, *113*, 6378−6396.

(62) Lee, C.; Yang, W.; Parr, R. G. Development of the Colle-Salvetti correlation-energy formula into a functional of the electron density. *Phys. Rev. B: Condens. Matter Mater. Phys.* **1988**, *37*, 785−789.

(63) Grimme, S. Semiempirical GGA-type density functional constructed with a long-range dispersion correction. *J. Comput. Chem.* **2006**, *27*, 1787−1799.

(64) Crich, D.; Vinogradova, O. Synthesis and Glycosylation of a Series of 6-Mono-, Di-, and Trifluoro S-Phenyl 2,3,4-Tri-O-Benzyl-Thiorhamnopyranosides. Effect of the Fluorine Substituents on Glycosylation Stereoselectivity. *J. Am. Chem. Soc.* **2007**, *129*, 11756−11765.

(65) Fang, T.; Gu, Y.; Huang, W.; Boons, G.-J. Mechanism of Glycosylation of Anomeric Sulfonium Ions. *J. Am. Chem. Soc.* **2016**, *138*, 3002−3011.

(66) Seeman, J. I. Effect of Conformational Change on Reactivity in Organic Chemistry. Evaluations, Applications, and Extensions of Curtin-Hammett Winstein-Holness Kinetics. *Chem. Rev.* **1983**, *83*, 83−134.

(67) Hammond, G. S. A. Correlation of Reaction Rates. *J. Am. Chem. Soc.* **1955**, *77*, 334−338.

(68) Walvoort, M. T. C.; Lodder, G.; Mazurek, J.; Overkleeft, H. S.; Codée, J. D. C.; van der Marel, G. A. Equatorial Anomeric Triflates from Mannuronic Acid Esters. *J. Am. Chem. Soc.* **2009**, *131*, 12080−12081.

(69) Yu, B.; Tao, H. Glycosyl Trifluoroacetimidates. 2. Synthesis of Dioscin and Xiebai Saponin I. *J. Org. Chem.* **2002**, *67*, 9099−9102.

(70) A 19F NMR was also acquired at low temperature of the newly formed intermediate upon addition of triflic acid to the glycosyl imidate. However, due to potential resonance overlap in the region previously reported for glycosyl triflates these resonances could not be definitively assigned (see Figure S11).

(71) van der Vorm, S.; Overkleeft, H. S.; van der Marel, G. A.; Codée, J. D. C. Stereoselectivity of Conformationally Restricted Glucosazide Donors. *J. Org. Chem.* **2017**, *82*, 4793−4811.

(72) Schumann, B.; Parameswarappa, S. G.; Lisboa, M. P.; Kottari, N.; Guidetti, F.; Pereira, C. L.; Seeberger, P. H. Nucleophile-Directed Stereocontrol Over Glycosylations Using Geminal-Difluorinated Nucleophiles. *Angew. Chem., Int. Ed.* **2016**, *55*, 14431−14434.

(73) D'Angelo, K. A.; Taylor, M. S. Borinic Acid Catalyzed Stereo- and Regioselective Couplings of Glycosyl Methanesulfonates. *J. Am. Chem. Soc.* **2016**, *138*, 11058−11066.

(74) Paulsen, H.; Stenzel, W. Bausteine von Oligosacchariden, X: Synthese α-1→4- und α-1→3-Verknüpfter Disaccharide der 2-Amino-2-Desoxy-D-Glucopyranose nach der Azid-Methode. *Chem. Ber.* **1978**, *111*, 2348−2357.

(75) Paulsen, H.; Stenzel, W. Bausteine von Oligosacchariden, IX: Stereoselektive Synthese α-Glycosidisch Verknüpfter Di- und Oligosaccharide der 2-Amino-2-Desoxy-D-Glucopyranose. *Chem. Ber.* **1978**, *111*, 2334−2347.

(76) Lemieux, R. U.; Ratcliffe, R. M. The Azidonitration of Tri-O-Acetyl-D-Galactal. *Can. J. Chem.* **1979**, *57*, 1244−1251.

(77) Nokami, T.; Shibuya, A.; Manabe, S.; Ito, Y.; Yoshida, J.-i. α- and β-Glycosyl Sulfonium Ions: Generation and Reactivity. *Chem. - Eur. J.* **2009**, *15*, 2252−2255.

(78) Crich, D.; Xu, H. Direct Stereocontrolled Synthesis of 3-Amino-3-Deoxy-Beta-Mannopyranosides: Importance of the Nitrogen Protecting Group on Stereoselectivity. *J. Org. Chem.* **2007**, *72*, 5183−5192.

(79) Crich, D. Mechanism of a Chemical Glycosylation Reaction. *Acc. Chem. Res.* **2010**, *43*, 1144−1153.